

Breakdown of Diffusion in Dynamics of Extended Waves in Mesoscopic Media

A. A. Chabanov,¹ Z. Q. Zhang,² and A. Z. Genack¹

¹*Department of Physics, Queens College of the City University of New York, Flushing, New York 11367, USA*

²*Department of Physics, Hong Kong University of Science and Technology, Clear Water Bay, Kowloon, Hong Kong*

(Received 28 November 2002; revised manuscript received 31 December 2002; published 22 May 2003)

We report the observation of nonexponential decay of pulsed microwave transmission through quasi-one-dimensional random dielectric media signaling the breakdown of the diffusion model. The decay rate of transmission falls nearly linearly in time corresponding to a nearly Gaussian distribution of the coupling strengths of quasinormal electromagnetic modes to free space at the sample surfaces. The peak and width of this distribution scale as $L^{-2.05}$ and $L^{-1.81}$, respectively.

DOI: 10.1103/PhysRevLett.90.203903

PACS numbers: 42.25.Dd, 05.60.-k, 42.25.Bs, 73.23.-b

The diffusion model is widely applied to electronic, neutron, and thermal conduction as well as to acoustic and electromagnetic propagation in multiply scattering media. The model is used not only when the phase of the wave is scrambled by inelastic scattering, but also in samples in which the wave is temporally coherent [1,2]. Since these samples are larger than the mean free path but smaller than the inelastic scattering length, we refer to them as mesoscopic. Although wave interference leads to large intensity fluctuations within a particular mesoscopic sample, the ensemble average of the flux reaching a point is generally assumed to be the incoherent sum of contributions of randomly phased, sinuating Feynman paths reaching that point. In this model, the average intensity varies smoothly in space and time and is governed by the diffusion equation.

Diffusion has been taken as the counterpoint to wave localization [3–5]. On one side are sharply defined localized modes with the average level spacing $\Delta\nu$ exceeding the typical level width $\delta\nu$, and on the other are diffusing waves for which $\delta\nu > \Delta\nu$ with $\delta\nu \sim D/L^2$, where D is the diffusion coefficient and L is the sample thickness [5]. However, the mode picture is inescapably a wave picture and at variance with particle diffusion in a number of respects. First, the diffusion equation is of first order, whereas the wave equation is of second order in time. The time evolution of the wave at any instant should therefore depend not only upon the spatial distribution of the particle density or intensity at that instant, as it does in the particle diffusion picture, but also on the previous history of the wave. Second, the particle picture represents the intensity as a discrete sum over diffusion modes, whereas the wave picture describes the field as a superposition of quasinormal modes with a continuum of decay rates in a random ensemble. The decay rates of the diffusion modes are given by $1/\tau_n = n^2 \pi^2 D / (L + 2z_0)^2$, where n is a positive integer and z_0 is the boundary extrapolation length. After a time τ_1 , the intensity distribution settles into the lowest diffusion mode and decays at a constant rate, $1/\tau_1$. In contrast, the decay rates of quasinormal modes in a random ensemble should be a

continuum. As time progresses, long-lived quasimodes would contribute more substantially and the rate of flow out of the sample would slow down continuously. Nonexponential decay has been observed in acoustic scattering in reverberant rooms [6] and solid blocks [7] as well as in microwave scattering in cavities whose underlying ray dynamics is chaotic [8]. Similarly, the decay rate of electronic conductance has been predicted to fall as a result of the increasing weight of long-lived, narrow-linewidth states [9]. The leading correction to the diffusion prediction for the electron survival probability $P_s(t)$ was calculated by Mirlin [10] using the supersymmetry approach [11] to be $-\ln P_s(t) = (t/\tau_1)(1 - t/2\pi^2 g \tau_1)$, where g is the dimensionless conductance [5], $g = \delta\nu/\Delta\nu$.

An ideal way to investigate the applicability of the diffusion model to mesoscopic systems is to consider pulsed electromagnetic transmission. Previous studies [12–15] have found exponential decay for $t > \tau_1$, as predicted by diffusion theory. However, measurements of optical transmission [14] indicate that the pulse rises earlier than predicted by diffusion theory. Even more puzzling is the finding by Kop *et al.* [15] of an increase in the inferred value of the diffusion coefficient with increasing L .

In this Letter, we report a dramatic breakdown of diffusion in microwave measurements in nominally diffusive random samples for which $\delta\nu > \Delta\nu$. We find that the decay rate of pulsed transmission falls nearly linearly in time, as predicted by Mirlin [10]. These results are interpreted in terms of the distribution of decay rates of quasimodes of the sample, which is found by taking the inverse Laplace transform of the decaying signal. The distribution of the modal decay rates is nearly Gaussian with an average value that scales as $L^{-2.05}$, which is close to the inverse square scaling for the decay rate in the diffusion model. The width falls as $L^{-1.81}$, which is faster than predicted by Ref. [10].

Spectra of the in- and out-of-phase components of the steady-state transmitted microwave field are measured in low-density collections of dielectric spheres using a

Hewlett-Packard 8772C vector network analyzer. These spectra are multiplied by a Gaussian envelope of width Δf centered at f_c and then Fourier transformed to give the response to a Gaussian pulse in the time domain. Conical horns are positioned 30 cm in front of and behind the sample. Linearly polarized microwave radiation is launched from one horn, and the cross-polarized component of the transmitted field is detected with the other to eliminate the ballistic component of radiation. The sample is composed of alumina spheres of diameter 0.95 cm and refractive index 3.14, contained within a 7.3-cm-diameter copper tube at an alumina volume fraction of 0.068 [16]. This low density is produced by embedding the alumina spheres within Styrofoam spheres of diameter 1.9 cm and refractive index 1.04. Measurements for random ensembles are obtained by momentarily rotating the tube about its axis to create new random configurations before each spectrum is taken. In this way, measurements are carried out in ensembles of 10 000 sample realizations at lengths of 61, 90, and 183 cm in samples A, B, and C, respectively. In addition, measurements are made in an ensemble of 2300 realizations of a more strongly absorbing sample of 90 cm length (sample D), produced by covering 40% of the inside surface of the tube with a strip of titanium foil laid from end to end. The measurements are made within the frequency interval 14.7–15.7 GHz for samples A, B, and D, and 15.0–15.4 GHz for sample C. The frequency intervals are chosen to be far from sphere resonances [16], so that the dynamics of transmission is uniform over the frequency range and the sample is far from the localization threshold. The closeness to localization, even in the presence of absorption, is indicated by the variance of the steady-state transmitted intensity normalized to its ensemble average value, $\text{var}(I/\langle I \rangle)$ [17]. In the absence of absorption, $\text{var}(I/\langle I \rangle) \simeq 1 + 4/3g$ [17,18]. At the localization threshold, $\text{var}(I/\langle I \rangle) \simeq 7/3$. The values of $\text{var}(I/\langle I \rangle)$ in samples A–D are 1.18, 1.26, 1.50, and 1.25, respectively.

The field of the temporal response to a Gaussian pulse peaked at $t = 0$ is squared to give the transmitted intensity $I(t)$ for each sample realization. The average transmitted intensity $\langle I(t) \rangle$ is found by averaging over the ensemble, and then over the frequency interval by shifting f_c . The results are shown on a logarithmic scale in Fig. 1(a). We find that, when $\Delta f > \delta\nu$, the tail of $\langle I(t) \rangle$ does not depend on Δf . We use $\Delta f = 15$ MHz for samples A, B, and D, and $\Delta f = 7.5$ MHz for sample C, so that $\Delta f > \delta\nu$ in all cases. The noise in the frequency spectra produces a constant background in the time domain. Once this background is subtracted, a dynamic range of more than 6 orders of magnitude is achieved. This makes it possible to study transmission on time scales an order of magnitude longer than the time of peak transmission, though the longest times are still smaller than the inverse level spacing, $1/\Delta\nu$, which gives

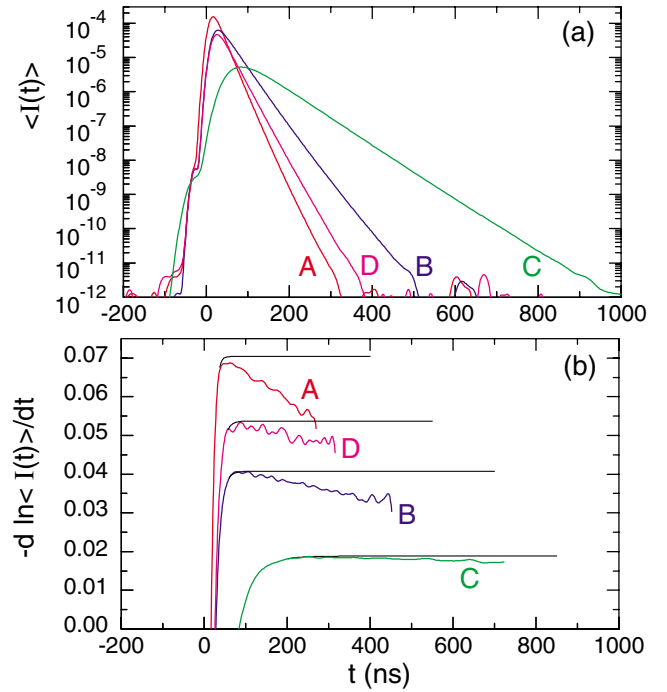


FIG. 1 (color online). (a) Average transmitted intensity in samples A–D. (b) Temporal derivative of the logarithm of the intensity gives the rate γ of the intensity decay due to leakage out of the sample and absorption. The thin black curves are the decay rates of the diffusion model with D^* , z_0 , and τ_a of Table I.

the time required for a photon to visit each coherence volume of the sample. The measured decay rate due to leakage out of the sample and absorption, $\gamma = -d \ln \langle I(t) \rangle / dt$, is plotted in Fig. 1(b). This rate is not constant as predicted by diffusion theory, but falls nearly linearly with time. The constant increase in the decay rate for sample D over that for sample B, seen in Fig. 1(b), indicates that the absorption rate $1/\tau_a$ and the leakage rate are additive. The decrease in γ with time is thus attributable solely to propagation out of the sample, which proceeds at a rate, $\gamma - 1/\tau_a = \pi^2 D(t) / (L + 2z_0)^2$. The absorption rate is found from a fit of the diffusion model [12–14] to measurements of $\langle I(t) \rangle$ up to the time at which 95% of the transmitted energy has passed through (Fig. 2). The fit is obtained by taking $D(t)$ to be a constant, D^* , and by minimizing the parameter $\chi^2 = (\sigma^2)^{-1} \sum [\langle I(t) \rangle_i - I(t_i)]^2$, where $\langle I(t) \rangle_i$ are the values of the measured intensity, σ is the uncertainty in $\langle I(t) \rangle_i$, averaged over the time of the fit, and $I(t_i)$ are the values of the model intensity [14] calculated at t_i . The parameters D^* , τ_a , and z_0 obtained from the fit are listed in Table I, and the corresponding decay rates are shown by the thin solid lines in Fig. 1(b). For sample A, χ^2 at the minimum depends only weakly on τ_a since the temporal range used in the fit is smaller than the τ_a . For this reason, we use the value $\tau_a = 97$ ns for this length, which is obtained in the fit to the data for sample C.

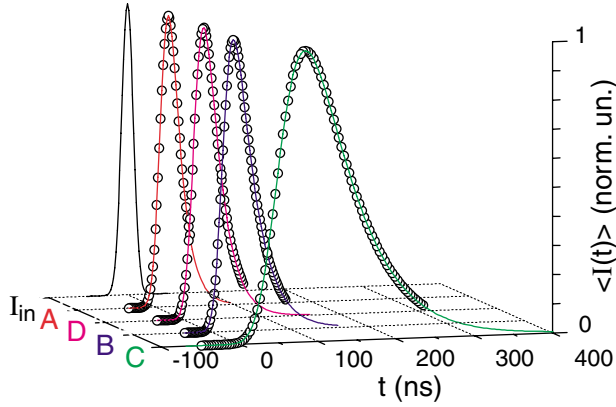


FIG. 2 (color online). Fit of the diffusion model to 95% of the full transmitted energy (circles) in samples A–D. The solid curves show the fit. I_{in} is the incident pulse of $\Delta f = 15$ MHz used to obtain A, B, and D; a pulse of $\Delta f = 7.5$ MHz was used to obtain D. All the curves are normalized.

The diffusion coefficient D^* obtained from the fit is found to decrease slightly with increasing L . The equality of the values of D^* and z_0 for samples B and D, seen in Table I, indicates that these parameters are not sensitive to the absorption rate. Moreover, when $1/\tau_a$ is subtracted from γ to give the decay rates without absorption in Fig. 3(a), the same time-dependent decay is found for both samples of 90 cm length.

The leakage rates in Fig. 3(a) give the “time-dependent diffusion coefficient,” $D(t) = (\gamma - 1/\tau_a)(L + 2z_0)^2/\pi^2$. The values of $D(t)$ found from the measurements may be compared to those from the theory of Ref. [10] for the survival probability, which yields $D(t) = D(1 - t/\pi^2 g\tau_1 + \dots)$. This is done by plotting $D(t)$ as a function of the dimensionless time $t' = t/g\tau_1$ in Fig. 3(b). The time $g\tau_1$ is proportional to $1/\Delta\nu$, and all the data are predicted to fall on a single curve. Although the data for samples with different values of L at a given time appear to coincide within the noise, there is a discernible decrease in the slope of $D(t')$ as L increases. As a result, the curves do not extrapolate to a constant bare diffusion coefficient at $t = 0$. When $D(t)$ is plotted instead versus the dimensionless time $t'' = t/\sqrt{g}\tau_1$ in Fig. 3(c), the slope

TABLE I. Values of the diffusion coefficient D^* , absorption time τ_a , and extrapolation length z_0 in samples A–D, obtained by fitting Eq. (1) of [14] to the short-time transmitted intensity of Fig. 2.

Sample	L (cm)	D^* (cm ² /ns)	τ_a (ns)	z_0 (cm)
A	61	39.4 ± 0.3	[97]	9.6 ± 0.3
B	90	37.9 ± 0.3	104 ± 7	9.8 ± 0.6
C	183	37.0 ± 0.8	97 ± 4	12.1 ± 2.5
D	90	37.4 ± 0.4	46 ± 2	8.7 ± 0.8

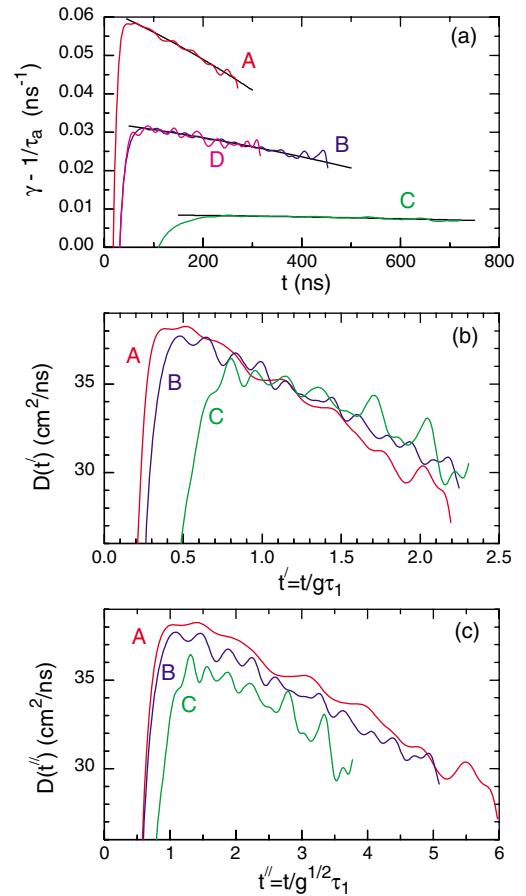


FIG. 3 (color online). (a) Leakage rates in samples A–D. The black curves are the best fit to the data by a polynomial of power 2. (b) “Time-dependent diffusion coefficients,” $D(t) = (\gamma - 1/\tau_a)(L + 2z_0)^2/\pi^2$, plotted versus $t' = t/g\tau_1$. (c) $D(t)$ plotted versus $t'' = t/\sqrt{g}\tau_1$.

of $D(t'')$ appears to be the same for all values of L ; however, the curves do not overlap. A strong deviation from exponential decay at $t'' \approx 1$ has also been found in numerical simulations [19].

The changing slope of $D(t)$ with L is associated with the scaling of the width of the distribution $P(\alpha)$ of decay rates of quasinormal modes of the sample. These are hypothesized to form a complete set [20], even when $\delta\nu > \Delta\nu$. Since the time evolution is given by the superposition of these modes [20], the average transmission can be expressed [7] as $\langle I(t) \rangle \propto \int_0^\infty P(\alpha) \exp(-\alpha t) d\alpha$. To find $P(\alpha)$, we use an approximate Laplace inversion algorithm based on the Weeks method [21]. A polynomial of power 2 is fit to the decay rates in Fig. 3(a). These fits are then used to compute curves $\langle I(t) \rangle$, which are inverted to obtain the distributions $P(\alpha)$ shown in Fig. 4. A linear decrease in $\gamma(t)$ with time as $\gamma(t) = a - bt$, $b/a \ll 1$, would correspond to a Gaussian distribution for $P(\alpha)$ with $\langle \alpha \rangle = a$ and $\text{var}(\alpha) = \sigma_\alpha^2 = b$. A departure of $P(\alpha)$ from a Gaussian form in Fig. 4 reflects a somewhat more rapid decay of $\gamma(t)$ in Fig. 3.

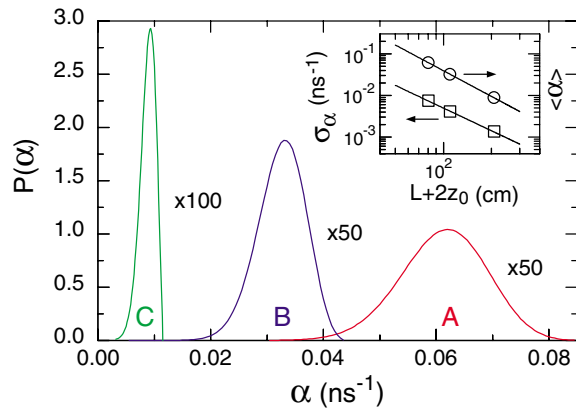


FIG. 4 (color online). Distribution of the modal decay rates, $P(\alpha)$, in samples A–C. Inset: scaling of the average $\langle\alpha\rangle$ (circles) and of the width σ_α (squares) of $P(\alpha)$, and the corresponding best fits to $\sim(L+2z_0)^\beta$ (solid) are shown on the log-log scale. The best fits are obtained with exponents of -2.05 and -1.81 for $\langle\alpha\rangle$ and σ_α , respectively.

The scaling of the average decay rate due to leakage out of the sample, shown in Fig. 4, is given by $\langle\alpha\rangle \propto (L+2z_0)^{-2.05}$. This is close to the inverse square scaling of the diffusion model and suggests that the dynamics observed is characteristic of extended waves and is not associated with the approach to localization with increasing L . The width of the distribution scales as $\sigma_\alpha \propto (L+2z_0)^{-1.81}$. This is close to the scaling, $\sigma_\alpha \propto \sqrt{b} \propto 1/g^{1/4}\tau_1 \propto L^{-1.75}$, and differs from the scaling predicted by Ref. [10], $\sigma_\alpha \propto \sqrt{b} \propto 1/\sqrt{g}\tau_1 \propto L^{-1.5}$.

The wide distribution of the modal decay rates in thin samples may be the source of the sharp spectral peaks observed in amplifying random media [22,23]. In these samples, lasing is initiated in the longest-lived modes, which have the lowest critical gain [24]. Such long-lived modes are expected to exhibit a sharply peaked spatial distribution.

In conclusion, we have found nonexponential decay of pulsed transmission through disordered media in which the level width exceeds the spacing between levels, even at long times and in thick samples. This departure from diffusion theory is interpreted in terms of the decay rate statistics of electromagnetic quasinormal modes. The statistics of these modes is fundamental to understanding the static and dynamic behavior of waves in both passive and active random media.

Discussions with X. Zhang, R. L. Weaver, T. Kottos, B. Shapiro, and B. A. van Tiggelen are gratefully acknowledged. This research is supported by the NSF Grant No. DMR0205186, U.S. ARO Grant No. DAAD190010362, and Hong Kong RGC Grant No. HKUST 6163/01P.

- [1] *Scattering and Localization of Classical Waves in Random Media*, edited by Ping Sheng (World Scientific, Singapore, 1990).
- [2] *Mesoscopic Phenomena in Solids*, edited by B. L. Altshuler, P. A. Lee, and R. A. Webb (North-Holland, Amsterdam, 1991).
- [3] P. W. Anderson, Phys. Rev. **109**, 1492 (1958).
- [4] E. Abrahams, P. W. Anderson, D. C. Licciardello, and T. V. Ramakrishnan, Phys. Rev. Lett. **42**, 673 (1979).
- [5] D. J. Thouless, Phys. Rev. Lett. **39**, 1167 (1977).
- [6] K. Bodland, J. Sound Vib. **73**, 19 (1980); F. Kawakami and K. Yamiguchi, J. Acoust. Soc. Am. **80**, 543 (1986).
- [7] J. Burkhardt and R. L. Weaver, J. Acoust. Soc. Am. **100**, 320 (1996); O. L. Lobkis, R. L. Weaver, and I. Rozhkov, J. Sound Vib. **237**, 281 (2000).
- [8] E. Doron, U. Smilansky, and A. Frenkel, Phys. Rev. Lett. **65**, 3072 (1990); H. Alt, H.-D. Gräf, H. L. Harney, R. Hofferbert, H. Lengeler, A. Richter, P. Schardt, and H. A. Weidenmüller, *ibid.* **74**, 62 (1995).
- [9] B. L. Altshuler, V. E. Kravtsov, and I. V. Lerner, in Ref. [2]; B. A. Muzykantskii and D. E. Khmelnitskii, Phys. Rev. B **51**, 5480 (1995).
- [10] A. D. Mirlin, Phys. Rep. **326**, 259 (2000).
- [11] K. B. Efetov, Adv. Phys. **32**, 53 (1983).
- [12] G. H. Watson, Jr., P. A. Fleury, and S. L. McCall, Phys. Rev. Lett. **58**, 945 (1987).
- [13] J. M. Drake and A. Z. Genack, Phys. Rev. Lett. **63**, 259 (1989); A. Z. Genack and J. M. Drake, Europhys. Lett. **11**, 331 (1990).
- [14] K. M. Yoo, F. Liu, and R. R. Alfano, Phys. Rev. Lett. **64**, 2647 (1990).
- [15] R. H. J. Kop, P. deVries, R. Sprink, and A. Lagendijk, Phys. Rev. Lett. **79**, 4369 (1997).
- [16] A. A. Chabanov and A. Z. Genack, Phys. Rev. Lett. **87**, 153901 (2001).
- [17] M. Stoytchev and A. Z. Genack, Phys. Rev. Lett. **79**, 309 (1997); A. A. Chabanov, M. Stoytchev, and A. Z. Genack, Nature (London) **404**, 850 (2000).
- [18] Th. M. Nieuwenhuizen and M. C. W. van Rossum, Phys. Rev. Lett. **74**, 2674 (1995); E. Kogan and M. Kaveh, Phys. Rev. B **52**, R3813 (1995).
- [19] G. Casati, G. Maspero, and D. L. Shepelyansky, Phys. Rev. E **56**, R6233 (1997).
- [20] E. S. C. Ching, P. T. Leung, A. Maassen van den Brink, W. M. Suen, S. S. Tong, and K. Young, Rev. Mod. Phys. **70**, 1545 (1998).
- [21] A. H.-D. Cheng, P. Sidauruk, and Y. Abousleiman, Mathematica J. **4**, 76 (1994).
- [22] H. Cao, Y. G. Zhao, S. T. Ho, E. W. Seelig, Q. H. Wang, and R. P. H. Chang, Phys. Rev. Lett. **82**, 2278 (1999).
- [23] S. V. Frolov, Z. V. Vardeny, and K. Yoshino, Phys. Rev. B **57**, 9141 (1998).
- [24] C. Vanneste and P. Sebbah, Phys. Rev. Lett. **87**, 183903 (2001); A. L. Burin, M. A. Ratner, H. Cao, and R. P. H. Chang, *ibid.* **87**, 215503 (2001); V. M. Apalkov, M. E. Raikh, and B. Shapiro, *ibid.* **89**, 016802 (2002); X. Jiang and C. M. Soukoulis, Phys. Rev. E **65**, 025601 (2002).